Ecological Indicators 117 (2020) 106593

Contents lists available at ScienceDirect

Ecological Indicators

journal homepage: www.elsevier.com/locate/ecolind

How quickly will the offshore ecosystem recover from the 2010 Deepwater Horizon oil spill? Lessons learned from the 1979 Ixtoc-1 oil well blowout

Melissa Rohal[a], Noe Barrera[a], Elva Escobar-Briones[b], Gregg Brooks[d], David Hollander[c], Rebekka Larson[d], Paul A. Montagna[a,*], Marissa Pryor[a], Isabel C. Romero[c], Patrick Schwing[c,d]

[a] Texas A&M University - Corpus Christi, Harte Research Institute for Gulf of Mexico Studies, 6300 Ocean Drive, Unit 5869, Corpus Christi, TX 78412, USA
[b] Universidad Nacional Autonoma de Mexico, Instituto de Ciencias del Mar y Limnologia, A.P. 70-305 Ciudad Universitaria, 04510 Mèxico, D.F, Mexico
[c] University of South Florida, College of Marine Science, 140 7th Ave S., St Petersburg, FL 33701, USA
[d] Eckerd College, 4200 54th Ave. S. Saint Petersburg, FL 33711, USA

ARTICLE INFO

Keywords:
Deepwater Horizon
Meiofauna
Macrofauna
Ixtoc
Oil spill

ABSTRACT

The Deepwater Horizon (DWH) accident occurred on 20 April 2010 in the Northern Gulf of Mexico and resulted in a deep-sea plume of petroleum hydrocarbons and a marine oiled snow sedimentation and flocculent accumulation (MOSSFA) event. It is hypothesized that recovery will occur when the contaminated sediment is buried below the biologically active zone of 10 cm. Recovery rate can be inferred from the similar Ixtoc-1 blowout and sub-surface oil release that occurred in the Bay of Campeche, Mexico in 1979 – 1980. In 2015, sediment chemistry effects from the Ixtoc-1 were found at 2.4– 2.8 cm sediment depth at stations within 81 and 273 km away. Trends of total polycyclic aromatic hydrocarbon concentration, macrofauna family-level diversity, and the nematode to copepod ratio with sediment depth supports the interpretation that the benthic community has not yet recovered from the Ixtoc-1 spill. Based on a sedimentation rate of 0.072 cm/year, the Ixtoc-1 benthic community will recover in 103 more years beyond 2015. Recovery around the DWH will occur in 50 years based on an average sedimentation rate of 0.2 cm/year. These rates demonstrate that benthic recovery in the deep sea is very slow.

1. Introduction

On 20 April 2010, the Deepwater Horizon (DWH) accident occurred in the northern Gulf of Mexico at a water depth of 1525 m. The benthic community was potentially exposed to an estimated 3.19 million barrels of oil residues (DWH Natural Resource trustees, 2016; Romero et al., 2017). Of all the oil released, up to 35% of the hydrocarbons were suspended in a deep-water plume that later is believed to have settled on the seafloor (Ryerson et al., 2012; Valentine et al., 2014; Romero et al., 2015; Romero et al., 2017). The formation of a Marine Oil Snow Sedimentation and Flocculent Accumulation event (MOSSFA) was observed as the result of the plankton and microorganisms stress responses to petroleum and dispersant exposure (Passow et al., 2012; Ziervogel et al. 2012; Passow, 2016; Daly et al., 2016). This resulted in increased concentrations of oil-residues in the deep-sea area with estimates ranging from 3200 (Valentine et al., 2014) to ~33,000 km^2 (Romero et al., 2015; Schwing et al., 2017). The impact on the benthic community is still severe with a 54% loss of macrofauna diversity and 38% loss of meiofauna diversity (Montagna et al., 2013). There was no recovery of this with reduced diversity four years after the spill (Reuscher et al., 2017). Based on what is known about deep-sea biology, it was argued that recovery could take many decades (Montagna et al., 2013). The purpose of the present study is to estimate recovery times for the DWH spill.

This exposure combination of direct oil residues and MOSSFA was observed during the Ixtoc-1 well blow out in the Bay of Campeche in the southwestern Gulf of Mexico (Jernelöv and Lindén, 1981). On June 3, 1979, in 51 m of water, high pressure build-up caused the Ixtoc-1 well to blow out and catch fire (Jernelöv and Lindén, 1981). The platform sank to the seafloor damaging the stack and well casing allowing the oil and gas to mix close to the seafloor (Jernelöv and Lindén, 1981). The spill continued until March 23, 1980 for 290 days resulting in about 475,000 metric tons (≈ 3.3 million barrels) of oil to be released (Jernelöv and Lindén, 1981). It was estimated that 1 – 3 million gallons (24 – 71 thousand barrels) of oil impacted the beaches and resided offshore in tar mats (Oil Spill Intelligence Reports, 1980). Oil moved to the north where a MOSSFA event likely occurred over deep-sea sediments (Sun et al. 2015; Vonk et al., 2015). The Ixtoc-1 and DWH

* Corresponding author.
E-mail address: Paul.Montagna@tamucc.edu (P.A. Montagna).

https://doi.org/10.1016/j.ecolind.2020.106593
Received 2 December 2019; Received in revised form 25 March 2020; Accepted 1 June 2020
Available online 29 June 2020
1470-160X/

oil spill share several similarities. Both spills occurred because of a buildup of high pressure, occurred close to the coast, occurred near important deltaic systems, and large amounts of dispersants were used (Jernelöv, 2010).

Because of the similarities between DWH and Ixtoc-1, the recovery rate of benthos around the location of the Ixtoc-1 accident can provide parameters that could be used to estimate the recovery of the DWH environment. The Gulf of Mexico is considered a large marine ecosystem unit (Yáñez-Arancibia and Day, 2004; Carlisle, 2014), and we do know how the gradients of benthic community structure and diversity are driven by temperature, salinity, depth, latitude, and longitude throughout the Gulf (Schwing et al., 2020). Two surficial sediment components of the benthic community, the macrofauna and the meiofauna, are often used as indicators of ecosystem health and therefore, are ideal organisms to study. These two groups represent two different size classes of microscopic animals that live on or in the sediment. Macrofauna are the larger of the two groups and are often retained on a 300 μm sieve while meiofauna are retained on 45 μm sieves (Montagna et al., 2017), but in deep-sea studies meiofauna are sometimes retained on 32 μm sieves (Giere, 2009) or 20 μm sieves (Danovaro 2010). Neither group can easily escape from disturbance because of their small size and relatively sedentary lifestyle. More importantly both groups have been used as indicators of the DWH deep-sea oil spill (Montagna et al., 2013; Baguley et al., 2015; Washburn et al., 2016). The damage of the deep sea surrounding the DWH site was caused by deposition of contaminants to surface sediments and a loss of diversity in the top 0 to 3 cm of the surface sediment (Washburn et al., 2016; Reuscher et al., 2017) Therefore, it is likely that benthic community recovery will occur when fresh, uncontaminated, sediment buries the contaminated sediment. The benthos are restricted to the top 8 to 10 cm of sediment in the Gulf of Mexico (Montagna et al., 2017), so it is likely that about 10 cm of fresh sediment must be deposited before there is complete recovery. It will take time for sediment to accumulate on the sea floor in the northern Gulf of Mexico, but the Ixtoc spill occurred in 1979 and sufficient time has passed to determine if this hypothesis is true. This hypothesis is tested by measuring the macrofauna and meiofauna community response and chemical contaminants at the Ixtoc-1 oil spill location vertically within the sediment. If there is an effect from the Ixtoc-1 oil spill in the southern Gulf of Mexico, we can then use sedimentation rates to predict recovery time at the DWH site in the northern Gulf of Mexico.

2. Methods

As part of the Center for the Integrated Modeling and Analysis of Gulf Ecosystems (C-IMAGE) II consortium research program, samples were collected from Jul 30th to August 9th, 2015 onboard the Universidad Nacional Autónoma de México's R/V Justo Sierra. Samples were collected with an Oktopus MUC 12–100 multiple corer in areas believed to have been impacted by the Ixtoc-1 oil according to Sun et al. (2015) (Fig. 1). Samples were collected within the fishery exclusion zone, with the closest station located 4 km south of the original Ixtoc-1 well head (Table 1). Three replicate cores with an inner diameter of 9.5 cm were collected from each station and sliced into 0 – 1, 1 – 3, 3 – 5, and 5 – 10 cm depth sections. Each section-sample was preserved in 7% formalin buffered with Borax© for processing in the lab. At each station water profiles with a CTD were collected. Only the deepest CTD measurements, which were at the bottom, were used for dissolved oxygen (DO), salinity, and temperature in the current study.

2.1. Fauna analyses

In the laboratory, the samples were rinsed over stacked 300 μm and 45 μm sieves to separate macrofauna and meiofauna respectively. The first replicate of each station for meiofauna was sorted in its entirety, but this took a week to a month to complete a sample; so the remaining meiofauna replicates were subsampled to complete the analyses within a day or two. The subsamples were separated into equal portions by sediment volumes of 25 or 33% depending on the sediment volume, thus only a portion of replicates 2 – 3 were sorted for each station and section for the meiofauna. The samples were sorted under a dissecting microscope and all macrofauna and metazoan meiofauna were counted and identified. Only the top two sections of the core were sorted, 0 – 1 and 1 – 3 cm, for the meiofauna because that is the sediment depth at which 87% of the meiofauna from 20 cm deep cores are located (Montagna et al., 2017). All macrofauna samples were retained on a 300 μm sieve for the 0 – 1, 1 – 3, 3 – 5, and 5 – 10 cm sections. About 97% of macrofauna occur in the top 10 cm of 20 cm deep cores (Montagna et al. 2017). The sections were sorted and identified to a major taxa level such as phylum, class, or order.

2.2. Geochronology

Long-term preservation of the DWH chemical signal in sedimentary systems has been identified (Romero et al., 2020), which means that it should be possible to identify the Ixtoc-1 signal in Bay of Campeche sediments. Short-lived radioisotope geochronologies, based on excess ^{210}Pb ($^{210}Pb_{xs}$) chronological analysis of cores from each station, were used to identify the vertical location within the sediment for the date of 1979–1980 using the methods described in Brooks et al. (2015) and Schwing et al. (2017). Additional evidence of the Ixtoc-1 signal was measured as Foraminifera calcite stable isotope proxies ($\delta^{13}C_{CaCO3}$) (Schwing and Machain-Castillo, 2020; Schwing et al., 2018) The sediment interval was identified based on three criteria: if depletion of stable carbon in Foraminifera was beyond natural variability, if depletion occurred during 1979–1980, and qualitatively, if the depletions identified as Ixtoc-1 in these cores were the same magnitude (0.3–0.4 per mil) as those documented for the three years following the DWH and which are now preserved below the surface of northern Gulf deep sediments.

2.3. Total polycyclic aromatic hydrocarbons (TPAH) concentrations

Sediment samples were freeze-dried (Labonco® 7,754,040 vacuum freeze-drier and 7,806,020 bulk tray) and ground to homogenization (Beriro et al., 2014; Romero et al., 2018). Extraction of samples was done using an Accelerated Solvent Extraction system (ASE 200®, Dionex; temperature: 100 °C, pressure: 1500 psi, and solvent mixture of 9:1 (v:v) hexane:dichloromethane). Deuterated surrogate PAHs standards (d_{10}-acenaphthene, d_{10}-phenanthrene, d_{10}-fluoranthene, d_{12}-benz(a)anthracene, d_{12}-benzo(a)pyrene, d_{14}-dibenz(ah)anthracene; Ultra Scientific ISM-750–1) were added to sediment samples prior to extraction. A one-step extraction and clean-up procedure was applied using ~ 1 g freeze-dried homogenized sample (Romero et al., 2018; Romero, 2019). Sediment extracts were concentrated to ~ 200 μl using a RapidVap (LABONCO RapidVap® Vertex™ evaporator model 73,200 series) and a gentle stream of nitrogen. Two extraction control blanks were included with each set of samples (15–20 samples). Prior to GC/MS analysis an internal standard was added to all samples (d_{14}-terphenyl; Ultra Scientific ATS-160-1). All solvents used were at the highest purity available.

One sediment sample was collected at each station, but the samples were split into three pseudoreplicates that were analyzed separately. For analysis of PAHs we followed modified EPA methods 8270D and 8015C, and QA/QC protocols. Analyses were carried in splitless injection mode on an Agilent 7680B gas chromatograph interfaced with an Agilent 7010 triple quadrupole mass spectrometer (GC/MS/MS) using a 30 m RXi-5sil column, UHP helium as the carrier gas, UHP argon gas to facilitate the dissociation of the precursor ions in the collision cell, and pressure at 1 mTorr, inlet temperature of 295 °C, constant flow rate of 1 ml/min, and MS detector temperature at 250 °C. GC oven temperature program was 60 °C for 2 min, 60 °C to 200 °C at a rate of 8 °C/min,

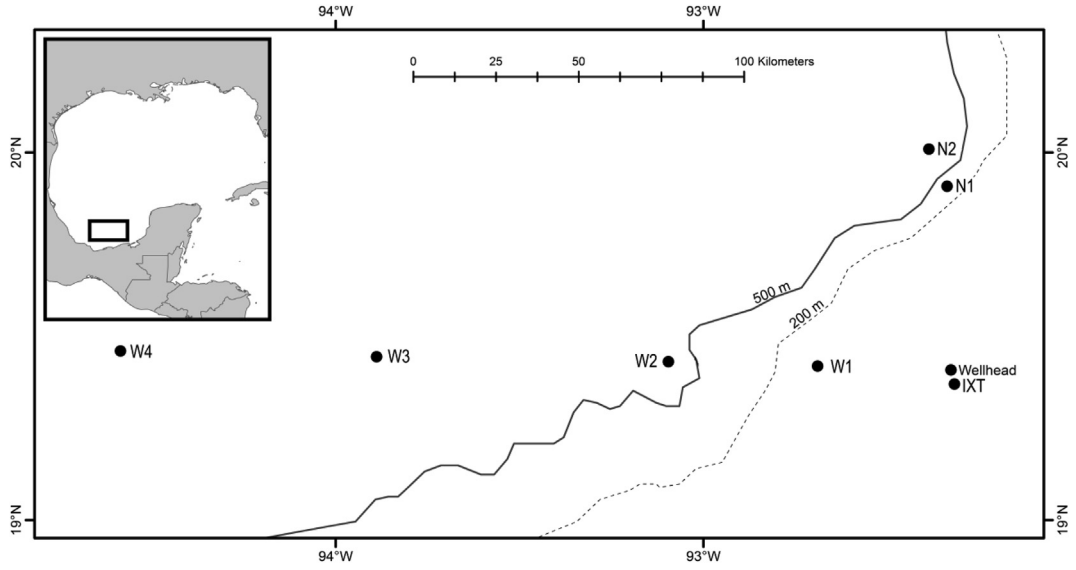

Fig. 1. Map of the sampling stations.

Table 1
Station location, distance (rounded to the nearest whole number) from the Ixtoc-1 wellhead, and depth.

Station	Latitude (degrees)	Longitude (degrees)	Depth (m)	Distance (km)	Direction	Label
IXTOC1	19.3701	−92.3172	60	4	–	IXT
IXW100	19.4187	−92.6894	179	38	W	W1
IXW250	19.4307	−93.0950	583	81	W	W2
IXW500	19.4442	−93.8887	1010	164	W	W3
IXW750	19.4600	−94.5849	1440	237	W	W4
IXN250	19.9080	−92.3373	779	56	N	N1
IXN500	20.0089	−92.3865	1240	67	N	N2

200 °C to 300 °C at a rate of 4 °C/min and held for 4 min, and 300 °C to 325 °C at a rate of 10 °C/min and held for 5 min. The GC/MS/MS was operated in Multiple Reaction Monitoring mode (MRM). Molecular ion masses for PAHs (precursor and product ions) were selected based on previous studies using GC–MS/MS-MRM (Sorensen et al., 2016; Adhikari et al, 2017; Van Eenennaam et al., 2018; Romero et al., 2018). Selected target compounds were: naphthalene and alkylated homologues; acenaphthylene, acenaphthene, fluorene, dibenzothiophene, phenanthrene and anthracene with their alkylated homologues, fluoranthene and pyrene with their alkylated homologues, benz[a]anthracene and chrysene with their alkylated homologues, benzo[b]fluoranthene, benzo[k]fluoranthene, benzo[a]pyrene, dibenz[a,h] anthracene, indeno[1,2,3-cd]pyrene, and benzo[ghi]perylene. For accuracy and precision of analyses we included laboratory blanks for every 10–14 samples, spiked controls for every 15–20 samples, tuned MS/MS to PFTBA (perfluorotributylamine) daily, included daily a standard reference material (NIST 2779). Recovery of individual PAHs ranged within QA/QC criteria of 50–120%. PAH concentrations are reported as recovery corrected. Each PAH analyte was identified using certified standards (Chiron S-4083-K-T, Chiron S-4406–200-T) and performance was checked using a 5-point calibration curve (0.04, 0.08, 0.31, 1.0 ppm). Quantitative determination of PAHs was conducted using response factors (RFs) calculated from the certified standard NIST2779. The limits of quantification (N = 10) ranged from 0.01 to 0.9 ng/g.

2.4. Statistical analyses

Univariate and multivariate analyses were performed using SAS 14.3 and Primer-e version 7 respectively. To correct for sorting subsamples of the meiofauna, abundance for vertical section subsamples was calculated by first averaging the count of each taxa in subsamples from a replicate core and then summing the averages together so that there would be one value per section per replicate. Before analysis all counts were scaled to the number of individuals/m^2. Community metrics of total abundance, Hill's N1 diversity, and richness were calculated for both macrofauna and meiofauna.

2.4.1. Univariate analysis

Univariate analysis of variance (ANOVA) was calculated with PROC GLM in SAS 14.3 (SAS, 2017). To test for differences among stations and vertical sediment depths (i.e., sections) the following dependent variables were used: square root transformed total abundance, total polycyclic aromatic hydrocarbons (TPAH), meiofaunal nematode abundance, copepod abundance, and the meiofaunal nematode to copepod ratio (NC). The NC ratio is an indicator of oil pollution at the DWH oil spill site (Montagna et al., 2013; Baguley et al., 2015). To test for differences with sediment depth a two-way partially hierarchical ANOVA was run across stations and sections. Because each replicate was split into sections, each section is from the unique replicates, thus sections are nested within the replicates, but each level of section occurs at each level of station, so these are crossed variable, thus a partially hierarchical design. The replicates are also a random variables, where as the stations and sections are fixed variables, thus a mixed model as well. The statistical model is $Y_{ijk} = \mu + \alpha_j + \beta_{k(j)} + \gamma_l + \alpha\gamma_{jl} + e_{ijkl}$ where Y_{ijk} is the dependent response variable, μ is the overall sample mean, α_j is the main fixed effect for stations, $\beta_{k(j)}$ is the random effect for replicates where $k = 1, 2,$ or 3; γ_l is the main fixed effect for sections where l = 0– 1, 1– 3, 3– 5,or 5– 10 cm, $\alpha\gamma_{jl}$ is the main fixed effect for the interaction between station and section, and e_{ijkl} is the random error term for each of the i replicate measurements within cells. The correct F-test for stations is to divide mean square of stations by the mean square of the replicates, all other treatments are divided by mean square error. Tukey's Honestly Significant Difference (HSD) test was run as a follow up comparison test. Degree of differences between statistically different samples was calculated by dividing the highest mean by the lowest. Meiofauna and macrofauna were analyzed in separate univariate and multivariate analyses because they are different groups.

2.4.2. Multivariate analysis

Primer-e version 7 software was used to analyze the benthic

community by considering the taxonomic groups and the number of individuals (abundance) within each group. To analyze across stations macrofauna and meiofauna were analyzed independently. The abundance data was square root transformed, then a resemblance matrix using Bray-Curtis similarity was created for the following analyses: A hierarchical CLUSTER analysis with group average, a SIMPROF test at a 5% significant level, and 999 permutations. A non-metric multi-dimensional scaling (nMDS) plot was generated with 1000 restarts and 0.01 minimum stress. A one-way ANOSIM was used to test for differences across stations. To determine which taxonomic group was driving the differences a one-way SIMPER analysis was run on the square root transformed abundance data and Bray-Curtis similarity was used to test for differences across stations and sediment sections.

A principal components analysis (PCA) was run on the environmental variables depth, DO, temperature, salinity, and Total PAHs in SAS 14.3. Prior to analysis, all variables were standardized to a normal distribution with a mean of zero and standard deviation of one so that all variables were on the same scale.

3. Results

3.1. Station trends

3.1.1. Environmental

There was little difference in salinity between stations but DO varied by up to 3.24 mg/L and temperature varied by up to 15 °C (Table 2). Chemical analysis of the hydrocarbon concentrations found that TPAH ranged from 43.74 to 156.37 ng/g across stations averaged across the top 10 cm (Table 2). Chronological analysis of benthic foraminifera stable carbon isotopes (Schwing and Machain-Castillo, 2020) identified a signal consistent with Ixtoc between 2.4 and 2.8 cm at W2 and from 2.4 to 2.6 cm at W4 (Table 2). A chronological analysis was not possible at stations IXT and W1 because the sediments were mixed and there was no stratification (Table 2). No Ixtoc signal was found at stations W3, N1, and N2.

Total PAH concentrations differed by station ($F_{6,24}$ = 14.96, P = < 0.0001) and section (i.e., sediment layer) ($F_{4,24}$ = 7.18, P = 0.0006) (Table 3). TPAH was 4 times higher at station IXT that was different from all other stations except W1 (Table 3). Section 0 – 1 was higher (up to 1.9 times higher) than sections 5 – 10 and 10 – 20 cm (Table 4).

Based on the environmental PCA, there are two groups of variables along the PC1 axis that represents high values of TPAH (identified as the presence of pollution), salinity, and temperature (depth) as positive values, and low dissolved oxygen and deep depths as negative values (Fig. 2A). PC1 accounted for 68% and PC2 accounted for 20% of the variation. The combination of pollution and depth occurs because stations IXT and W1 had the highest TPAH concentrations but were also the shallowest and warmest waters (Fig. 2B). The vertical sections within stations group together, but stations are separate, meaning there is more similarity within sediment depths at a station than among the stations (Fig. 2B). Only the two furthest and deepest stations, N2 and W3, overlap and appear to be similar.

Table 2
Environmental measurements at each station. Bottom water, and sediment total polycyclic aromatic hydrocarbon (TPAH) average total concentration from 0 to 10 cm. The depth of the Ixtoc signal is estimated from values derived from stable carbon isotope measurements from benthic Foraminifera (Schwing and Machain-Castillo, 2020).

Station	Dissolved Oxygen (mg/L)	Temperature (°C)	Salinity (PSU)	TPAH (ng/g)	Depth of Ixtoc Signal
IXT	3.27	19.95	36.43	156.37	Mixed
W1	2.82	15.58	36.04	146.84	Mixed
W2	2.59	8.27	35.03	102.13	2.4 – 2.8 cm
W3	4.05	5.20	34.93	84.73	No Signal
W4	5.61	4.27	34.97	43.74	2.4–2.6 cm
N1	4.02	6.60	34.93	84.86	No Signal
N2	5.83	4.56	34.96	115.60	No Signal

3.1.2. Macrofauna

Macrofauna and meiofauna community metrics were compared in the top 3 cm of sediment (Table 4). The highest macrofauna average abundance was at IXT (60 m), as much as 8.8 times higher, which also had the lowest diversity, as much as 1.9 times lower. The lowest macrofauna richness was at N2 (1240 m), as much as 1.8 times lower.

The nMDS and CLUSTER analysis for macrofauna across all sediment sections found IXT (60 m) was different from all other stations at 52% similarity (Fig. 3). The one-way ANOSIM across stations confirmed a difference between stations (R = 0.664, P = 0.001, n = 19). The one-way SIMPER analysis found that the differences between stations was attributed to 6 different taxonomic groups the isopod *Asellota*, polychaetes, oligochaetes, nematodes, amphipods, and tanaids. There was not one group that dominated the differences between all stations.

3.1.3. Meiofauna

Meiofauna average abundance and diversity was highest at IXT (60 m), as much as 3.2 and 1.3 times higher respectively, while richness was highest at W1 (179 m), as much as 2 times higher (Table 5). The lowest diversity and richness was at W3 (1440 m). Total abundance (square root transformed) differed by station ($F_{6,24}$ = 5.36, P = 0.0067) and section ($F_{1,24}$ = 12.53, P = 0.0041). Abundance in IXT was up to 3.2 times higher than W1, N2, W1, W3 and W2.

The nMDS and CLUSTER analysis for meiofauna in the top 3 cm found that IXT was different from all other stations except N1 replicate 2 at 60.83% similarity (Fig. 4). Stations W1 was different from stations N1, N2, W1, W2, and W3 at 72.48% (Fig. 4). The one-way ANOSIM across stations confirmed a significant difference between stations (R = 0.569, P-value = 0.001, n = 19). The one-way SIMPER analysis found that nematodes were the taxonomic group contributing the most to differences between stations, with nematodes contributing up to 25.73% of the dissimilarity and the highest abundances at IXT. For 6 of the 21 comparisons the highest contributing groups were either nauplii or gastrotrichs.

3.2. Sediment depth trends

3.2.1. PAh

Even though the station*section interaction was not significant (Table 3), the section with the highest concentration varied by station, with the highest (up to 6.3 times higher) found from 3 to 5 cm at station W1 (Fig. 5).

3.2.2. Macrofauna

Average total macrofauna abundance (square root transformed) differed by station ($F_{6,12}$ = 10.26, P = 0.0004) and section ($F_{3,36}$ = 15.06, P = < 0.0001) (Table 5). With the abundance at IXTOC1 being higher (up to 2.5 times higher) than all others (Fig. 6 and Table 5). Abundance in section 0 – 1 cm was higher (up to 1.8 times higher) than sections 3 – 5 and 5 – 10 cm (Fig. 6 and Table 5).

Hill's N1 diversity and richness was different by section only ($F_{3,48}$ = 6.52, P = 0.0012 and $F_{3,48}$ = 15.60, P = < 0.0001 respectively) (Table 5). Diversity was up to 1.7 times higher in section 0 – 1 cm than sections 3 – 5 and 5 – 10 cm (Table 5). Richness was higher (up to 2.3 times higher respectively) in the top two sections 0 – 1 and 1 – 3 cm compared to the bottom two (Fig. 7).

At stations N1, N2, and W1 section 3 – 5 cm when abundance, diversity, and richness was lowest TPAH concentrations were highest (Figs. 6,7).

Table 3
Analysis of variance results for differences among TPAH (ng/g) means by station and section. A) ANOVA table. B) Tukey HSD groupings for TPAH concentrations by station where underlined values are < 0.05. C) Tukey HSD groupings for TPAH concentrations by section.

A)

Source	DF	F Value	Pr > F
Station	6	14.96	<.0001
Section	4	7.18	0.0006

B)

Mean	158.49	136.37	99.83	93.01	78.37	77.65	39.27
Station	IXT	W1	N2	W1	W2	N1	W3

C)

Mean	129	108	98.9	83.6	68.3
Section	0 - 1	3 - 5	1 - 3	5 - 10	10 – 14.5

3.2.3. Meiofauna

Total abundance (square root transformed) differed by station ($F_{6,12}$ = 5.36, P = 0.0067) and section ($F_{1,\ 12}$ = 12.53, P = 0.0041) (Table 5). Section 0 – 1 cm was significantly 1.2 times higher than the 1 – 3 cm section (Fig. 8). For Hill's N1 diversity station ($F_{6,12}$ = 3.12, P = 0.0441), section ($F_{1,12}$ = 150.19, P = < 0.0001), and the station*section interaction ($F_{6,124}$ = 4.84, P = 0.0099) was significant (Table 5). Richness differed by station ($F_{6,12}$ = 3.31, P = 0.0369) and section ($F_{1,12}$ = 114.51, P = < 0.0001) (Table 5). W1 had a higher richness (up to 2 times higher) than W2, N2, W1, and W3 (Fig. 9). Richness was highest in the top 1 cm (up to 1.7 times higher) (Fig. 9). Nematode abundance was significantly different by station ($F_{6,12}$ = 5.04, P = 0.0084) (Table 6). Nematode abundance was higher (up to 3.4 times higher) at IXT than W1, N2, W1, W3, and W2 (Table 6). Copepod abundance differed by section ($F_{1,\ 12}$ = 117.8, P = < 0.0001) with a significant station*section interaction (F = 3.85, P = 0.0224). Copepod abundance was higher (up to 3.8 times higher) in the 0 – 1 cm section (Table 6). The NC ratio was different by station ($F_{6,\ 12}$ = 16.15, P = < 0.0001), section ($F_{1,\ 12}$ = 115, P = < 0.0001), and the station*section interaction was significant ($F_{6,12}$ = 8.22, P = 0.0011)

Table 4
Two-way partially hierarchical ANOVA results for macrofauna square root total abundance, Hill's N1 diversity, and richness across stations and section. A) ANOVA table. B) Tukey HSD test results for abundance by station. C) Tukey HSD test results for abundance by section. D) Tukey HSD test for diversity by section. E) Tukey HSD test results for richness by section.

A)		Abundance		Diversity		Richness	
Source	DF	F Value	Pr > F	F Value	Pr > F	F Value	Pr > F
Station	6	10.26	0.0004	1.42	0.2333	2.61	0.0745
Replicate(Station)	12	1.13	0.3708	0.98	0.4845	0.72	0.7260
Section	3	15.06	<0.0001	6.52	0.0012	15.60	<0.0001
Station*Section	18	1.34	0.2201	0.88	0.6064	0.68	0.8029

B)

				Abundance			
Mean	83.5	55.2	52.2	44.1	39.1	38.1	33.9
Station	IXT	W1	W1	N1	W2	N2	W3

C)

		Abundance		
Mean	66.4	59.4	37.9	35.9
Section	0 - 1	1 - 3	5 - 10	3 - 5

D)

		Diversity		
Mean	4.53	3.66	2.82	2.7
Section	0 - 1	1 - 3	5 - 10	3 - 5

E)

		Richness		
Mean	7.16	5.53	3.63	3.16
Section	0 - 1	1 - 3	5 - 10	3 - 5

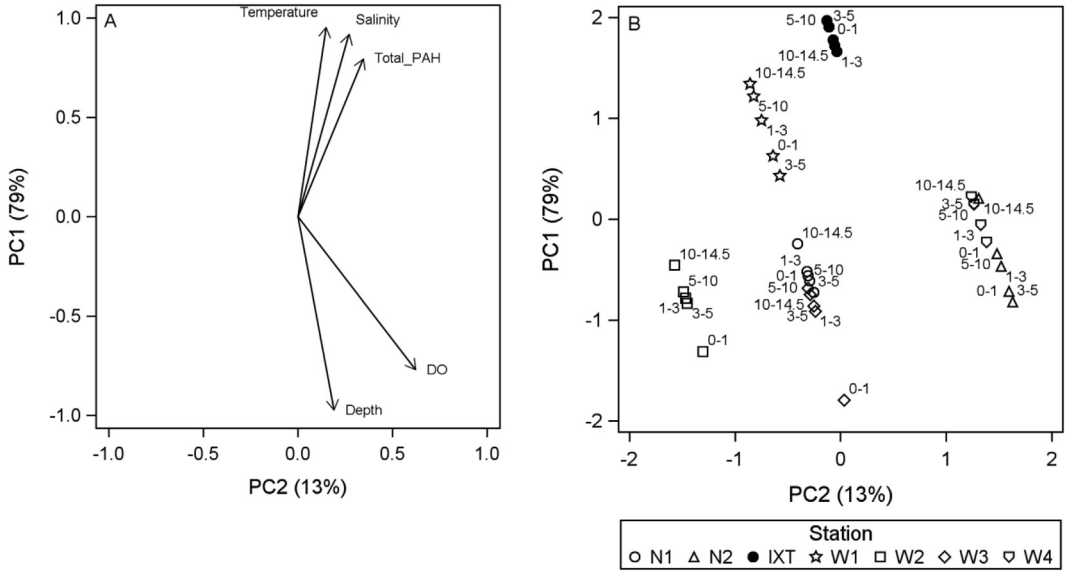

Fig. 2. Principal components analysis of the environmental variables measured at each station. A) Variable vector loads. B) Sample scores for sediment section depths at stations.

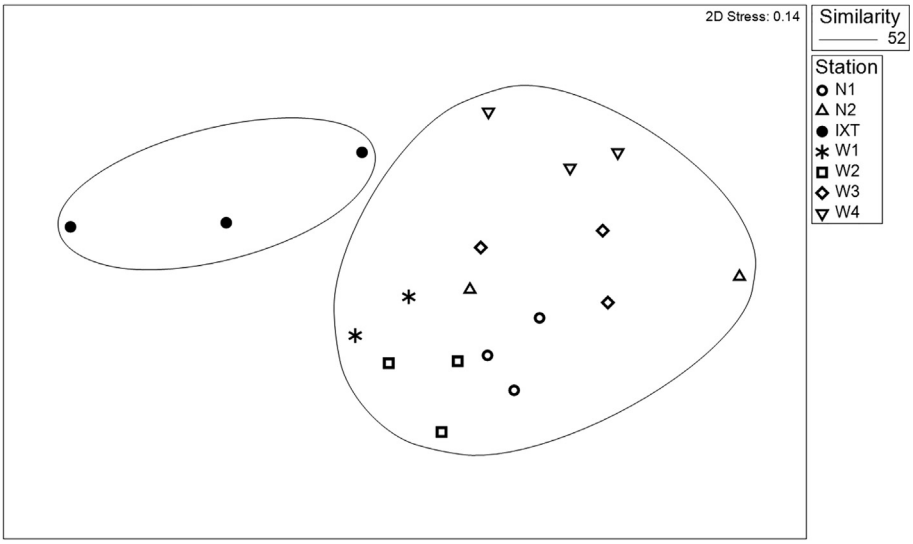

Fig. 3. A nMDS plot of differences among replicates within stations based on the macrofauna community structure integrated by sediment depth. The lines represent samples that share the same percent similarity.

(Table 6 and Fig. 10). The interaction occurred because of an increased difference in NC between sections at IXT (8.9 times higher in 1 – 3 cm) and a decreased difference in sections at station W2 (0.98 times higher in 1 – 3 cm). For all but station IXT richness was high when TPAH was high.

4. Discussion

The premise of this study is that the vertical distribution of sediments provides a chronological record that reflects information about past events. It is assumed that the area around the DWH wellhead will recover once the contaminated sediment is buried below the biologically active zone of 10 cm based on vertical distributions of macrofauna and meiofauna in studies of baseline sites (Montagna et al., 2017). The Ixtoc-1 spill, which occurred 36 years prior to the current sampling, provides a test case for determining if the chronology premise is correct, so the approach could be used to estimate the recovery rate of the DWH impact area. However, an important assumption of this study is that the sediment remains vertically laminated so that layers can be identified at depths that represent different time frames. Finally, chemical and biological data must be considered together because as the assessment is to determine if biological metrics are changing in response to chemical metrics.

There is an important difference between the two spills, because the DWH affected benthos are in the deep sea, but the Ixtoc affected benthos span great depth ranges. The Ixtoc plume moved to the west, and therefore moved over great depth ranges (Sun et al. 2015). So, whereas the DWH depths remain deep-sea in nature, the Ixtoc depths range from shallow to deep. The sampling stations (Table 1) were chosen based on the results provided by Sun et al. (2015). Depth is thus a confounding factor in the current study, because benthic community structure is known to change with depth. Additionally, it is possible that shallow areas would have sediments that are vertically mixed by waves or currents.

Of the seven stations sampled, W1 and IXT were classified as having the shallowest water depth (179 and 60 m respectively), highest

Table 5
Two-way partially hierarchical ANOVA results for meiofauna square root total abundance, Hill's N1 diversity, and richness across stations and section. A) ANOVA table. B) Tukey HSD test results for abundance by station. C) Tukey HSD test results for richness by station. D) Tukey HSD test results for diversity by station. E) Tukey HSD test results for abundance by section. F) Tukey HSD test results for diversity by section. G) Tukey HSD test results for richness by section.

A)		Abundance		Diversity		Richness	
Source	DF	F Value	Pr > F	F Value	Pr > F	F Value	Pr > F
Station	6	5.36	0.0067	3.12	0.0441	3.31	0.0369
Replicate(Station)	12	2.26	0.0857	1.05	0.4681	3.68	0.0161
Section	1	12.53	0.0041	150.19	<0.0001	114.51	<0.0001
Station*Section	6	1.45	0.2731	4.84	0.0099	3.26	0.0386

B)	Abundance						
Mean	761,000	528,000	291,000	272,000	264,000	240,000	238,000
Station	IXT	N1	W1	N2	W1	W3	W2

C)	Richness						
Mean	27	23.7	18.8	17.8	17.3	16.7	13.8
Station	W1	IXT	N1	W2	N2	W1	W3

D)	Diversity						
Mean	2.93	2.69	2.43	2.41	2.30	2.27	2.23
Station	IXT	W2	W1	N1	W1	N2	W3

E)	Abundance	
Mean	640	536
Section	0 - 1	1 - 3

F)	Diversity	
Mean	3.18	1.79
Section	0 - 1	1 - 3

G)	Richness	
Mean	23.8	14.2
Section	0 - 1	1 - 3

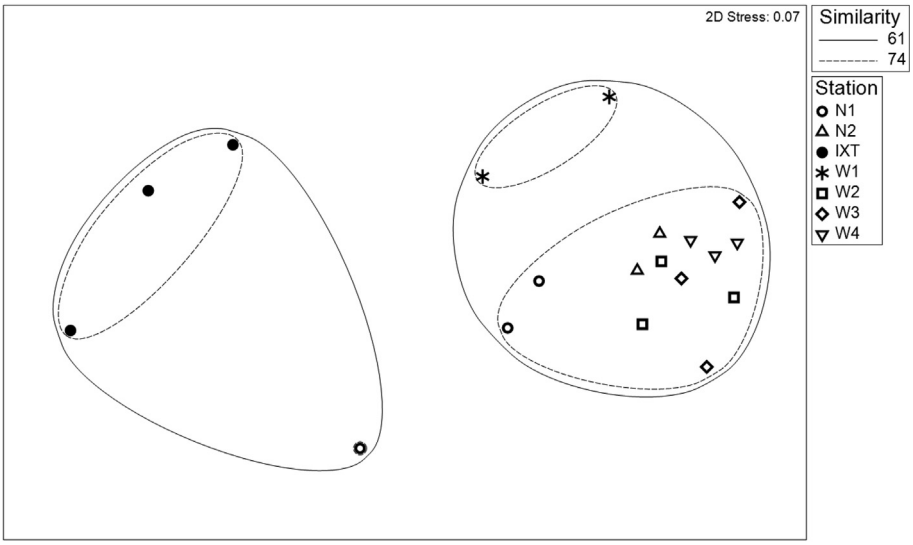

Fig. 4. A nMDS plot differences among replicates within stations based on the meiofauna community integrated by sediment depth. The lines represent samples that share the same percent similarity.

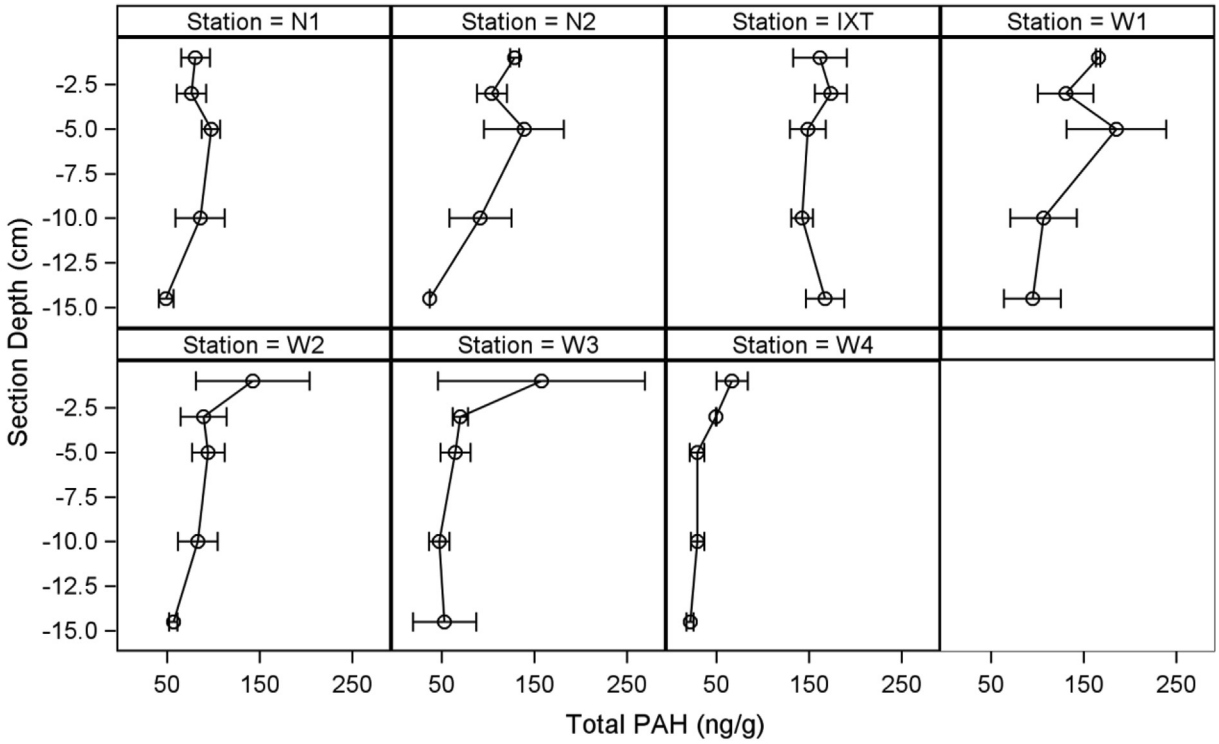

Fig. 5. Total PAH concentration across stations by sediment core sections. Boxes indicate the location of highest concentrations at each station.

temperature, highest salinity, and highest TPAH concentration compared to the other stations (Table 2 and Fig. 2B). Therefore, TPAH concentration is correlated with all these variables (inversely by water depth, and positively with temperature and salinity) along PC1 (Fig. 2A). However, it is interesting that IXT has the highest TPAH concentration (Tables 2 and 3) because this may be a remnant of the Ixtoc-1 oil spill, or continuous seeping from nearby seeps, or continued petroleum production activity in the area. The IXT station is closest to the original wellhead location, but the trend observed in the mixed sediments indicates PAHs main source might be from petroleum production activity. The Campeche Bay area is still an active petroleum production area and W1 and IXT are closest to the ongoing oil and gas production (Fig. 11), which would confound any Ixtoc-1 chemical signals and biological effects. However, the highest concentrations of

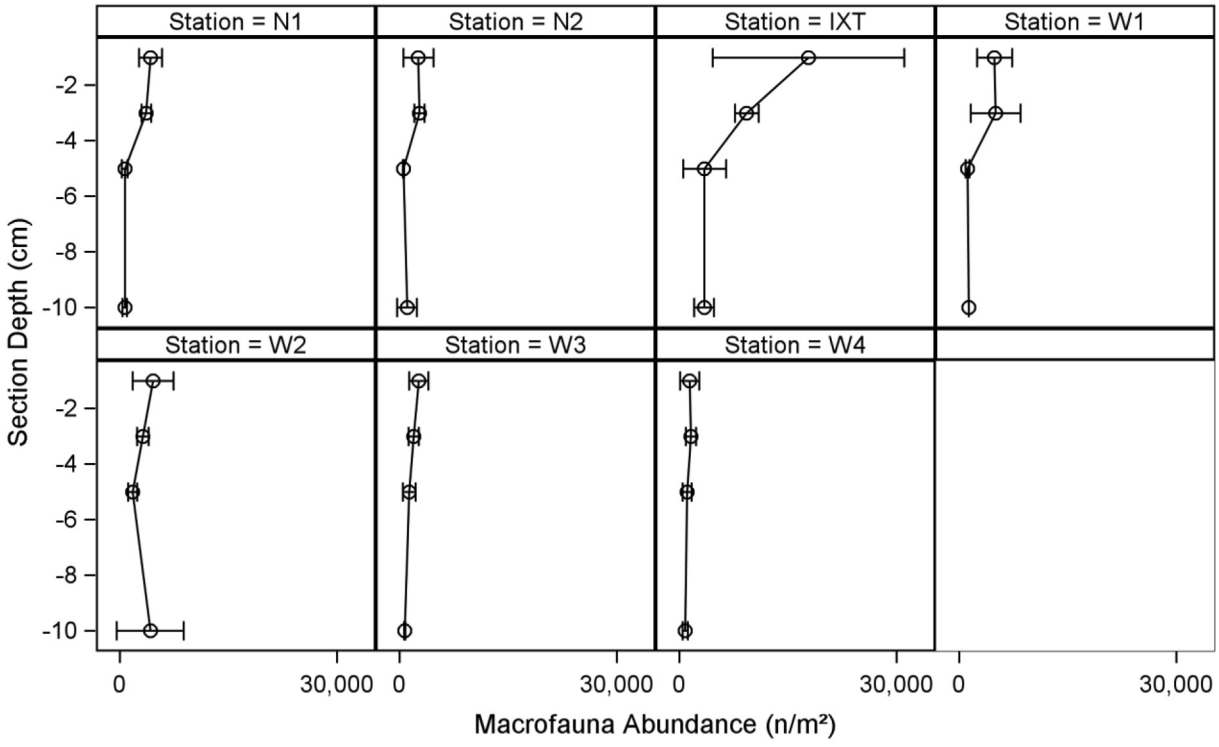

Fig. 6. Total untransformed macrofauna average abundance across stations by sediment core sections.

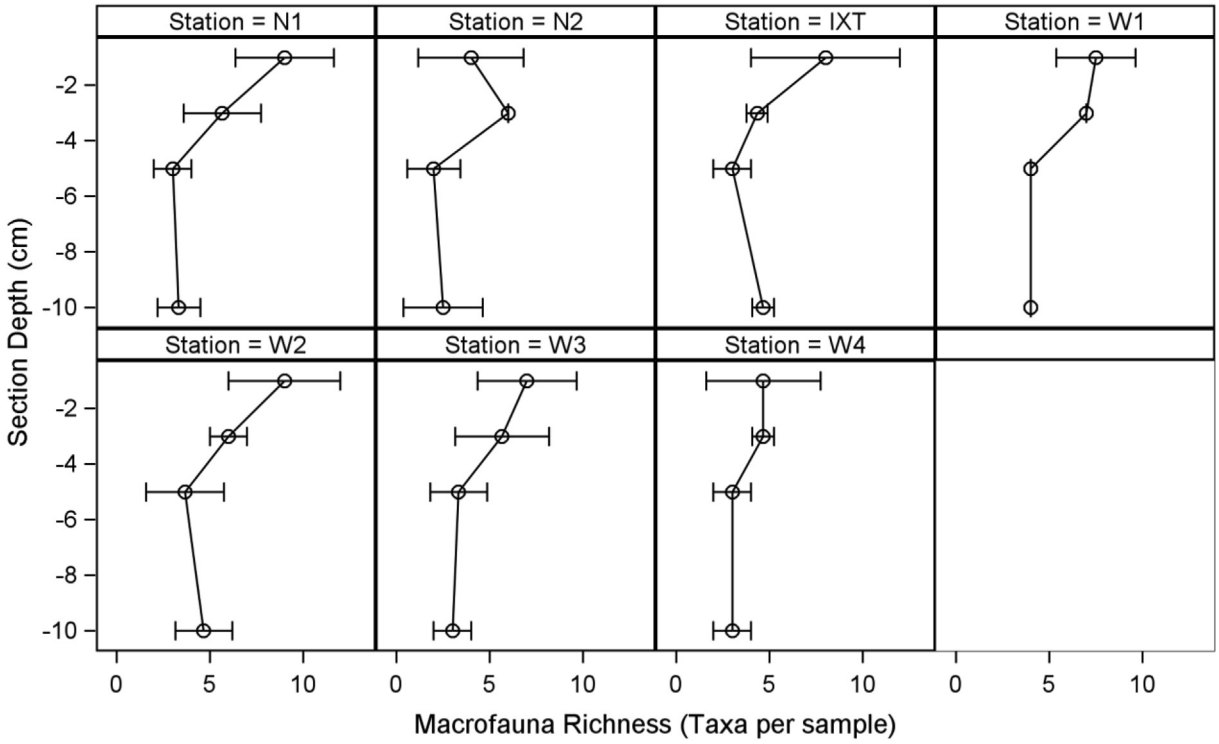

Fig. 7. Macrofauna taxa richness across stations by sediment core sections.

TPAHs were found in the 3 – 5 cm and 1 – 3 cm sections respectively and not on the surface (Fig. 5). The elevated levels at these sediment depths below the surface could be from the Ixtoc-1 oil spill because a signal was found from 2.4 to 2.8 cm depth at two other stations, which is close to the depths of elevated TPAH levels (Table 2, Fig. 5).

The TPAH concentrations in the area are low compared to other regions and sediment quality standards. The highest TPAH concentration of 173 ppb, at station IXT 1–3 cm, was not far above the median value of 92 ppb for background TPAH concentrations in the northern Gulf of Mexico (Wade et al., 2008). The Ixtoc-1 area TPAH values are below the sediment quality minimum effects range developed for nearshore benthic fauna of 4022 ppb (Long et al., 1995). However, it can't be assumed that shallow water animals have the same sensitivity as deeper living animals. Shallow water environments, like

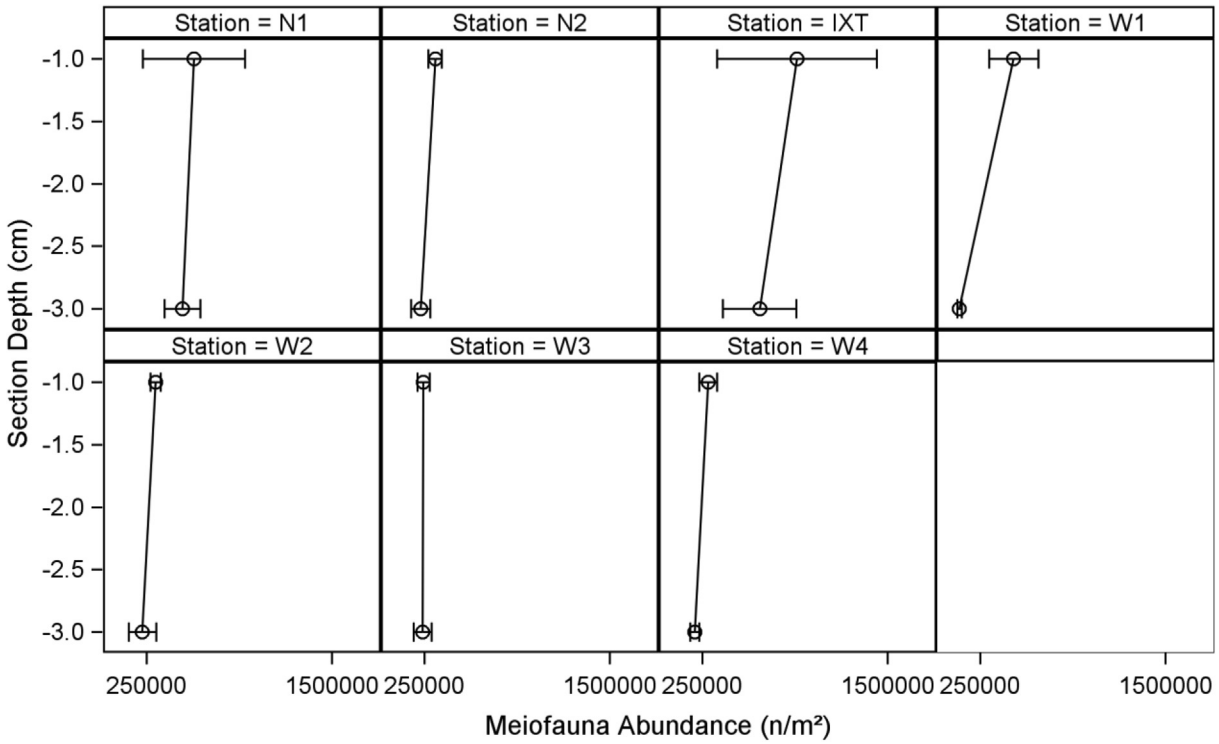

Fig. 8. Average total meiofauna abundance across stations by sediment core sections. Stations are in order of orientation and distance from wellhead.

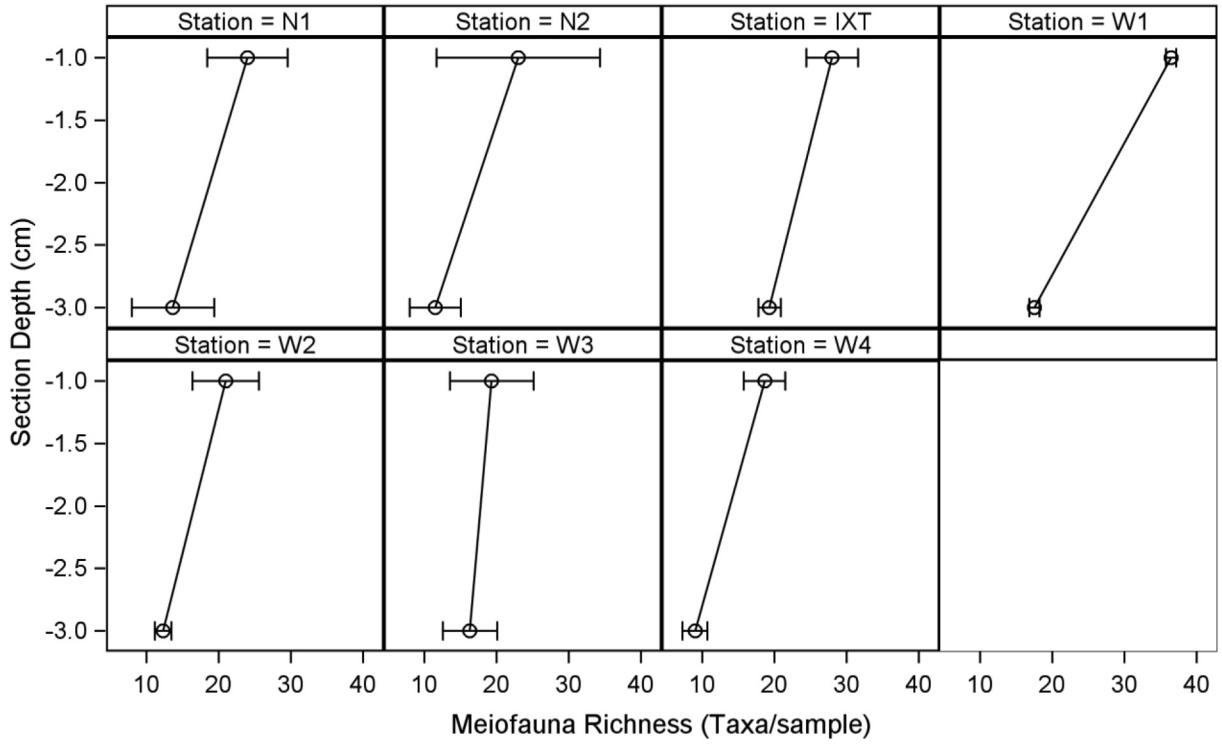

Fig. 9. Average meiofauna richness across stations by sediment core sections. Stations are in order of orientation and distance from wellhead.

Table 6
Two-way partially heirarchial ANOVA results for nematode abundance, copepod abundance, and the nematode copepod ratio (NC). All square root transformed.

A)		Nematode		Copepod		NC	
Source	DF	F Value	Pr > F	F Value	Pr > F	F Value	Pr > F
Station	6	5.04	0.0084	3.24	0.0394	16.15	<0.0001
Replicate(Station)	12	2.26	0.0861	1.11	0.4288	1.28	0.3397
Section	1	3.91	0.0715	117.80	<0.0001	115.00	<0.0001
Station*Section	6	1.46	0.2722	3.85	0.0224	8.22	0.0011

B)				Nematode			
Mean	657,000	454,000	247,000	229,000	208,000	204,000	193,000
Station	IXT	N1	W1	N2	W1	W3	W2

C)				NC			
Mean	36.5	17.7	16.8	9.42	8.57	8.36	5.61
Station	IXT	W1	N1	W3	W1	N2	W2

E)	Diversity	
Mean	3.18	1.79
Section	0 – 1	1 – 3

F)	Copepod	
Mean	62,400	16,300
Section	0 – 1	1 – 3

G)	NC	
Mean	23.8	6.00
Section	1 – 3	0 – 1

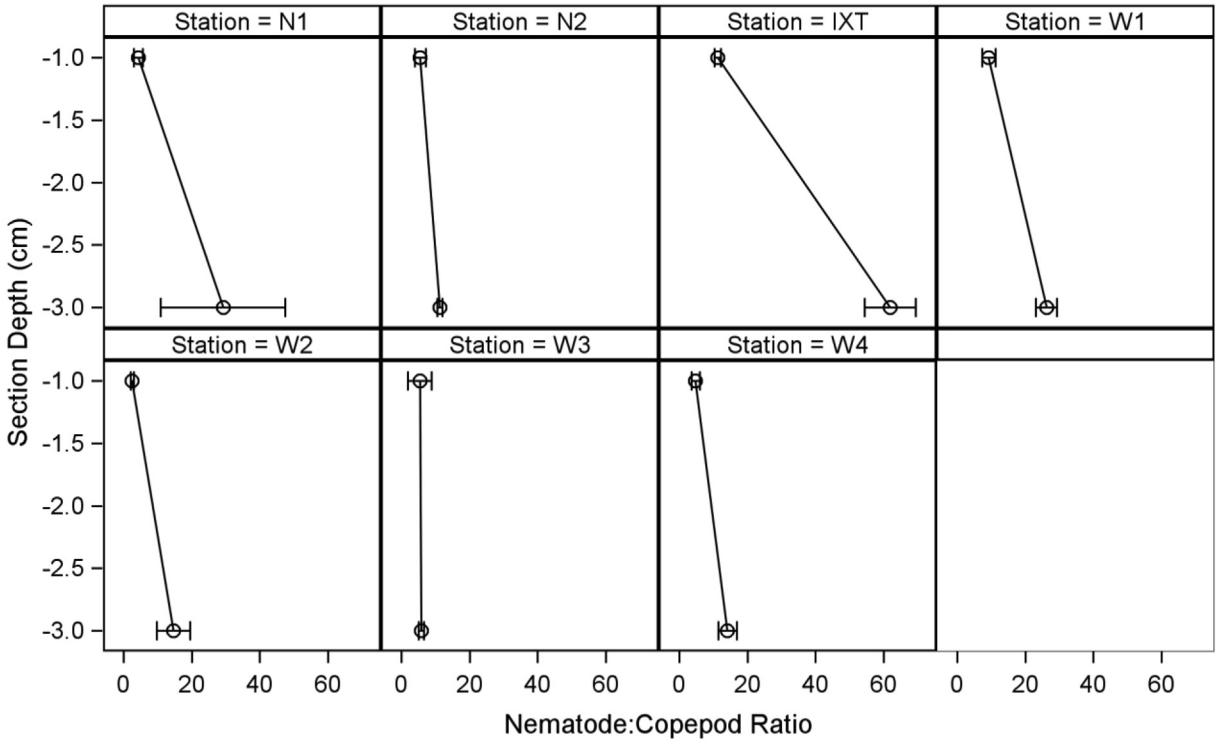

Fig. 10. Average nematode copepod ratio (NC) across stations by sediment depth sections. Stations are in order of orientation and distance from wellhead.

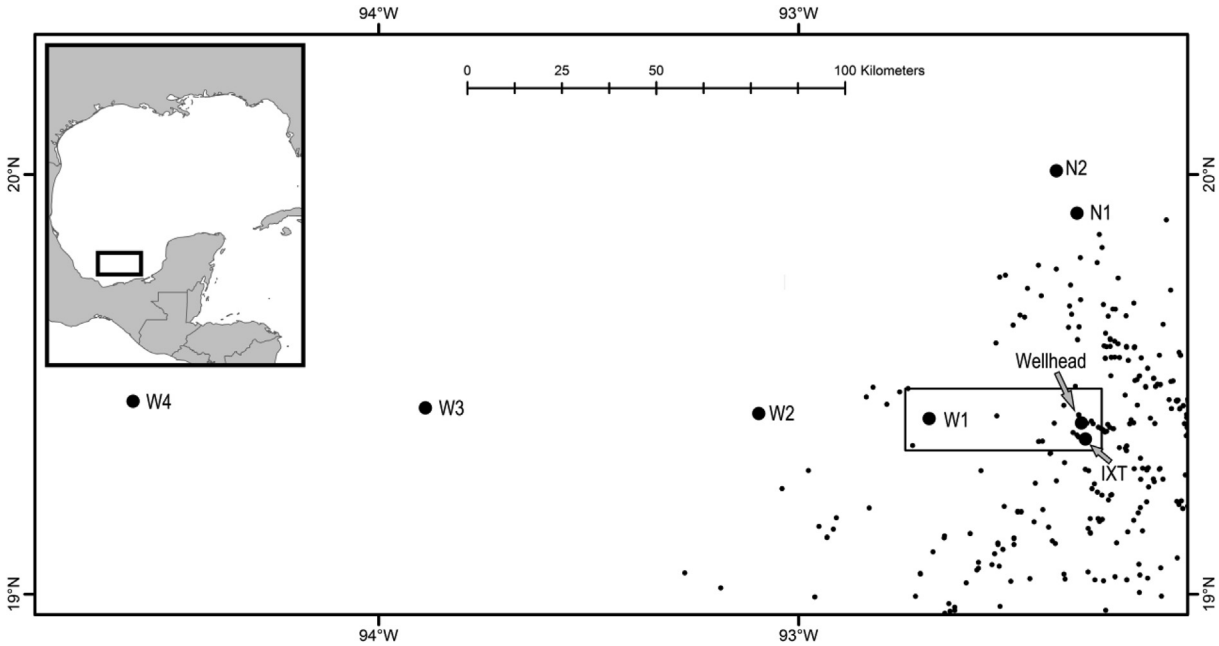

Fig. 11. Map showing the location of the sample stations (large circles, station names in Fig. 1) and shallow wells (small circles). Box = W1, IXT, and Ixtoc-1 wellhead.

the coastal areas of the Gulf of Mexico, have an order of magnitude higher PAH concentrations than offshore continental shelf sediments (Kennicutt et al., 1996). Field observations following the DWH found moderate benthic effects (i.e., a 5% loss of macrofauna diversity and a 19% loss of meiofauna diversity) starting at 370 ppb (Montagna et al., 2013; Baguley et al., 2015). The average PAH value in the DWH impacted zones where benthic community effects are still being observed after four years was 218 ppb (Reuscher et al., 2017). Estuarine organisms that are always exposed to higher concentrations could be more tolerant of PAH than offshore organisms. In addition, the animals around the Ixtoc oil spill site have been undergoing chronic exposure. The sediment quality standards proposed by Long et al. (1995) are all based on acute exposure. None of the studies reviewed ran for longer than 4 months (Long et al., 1995), the Ixtoc oil spill occurred over 30 years ago. Therefore, even though the PAH levels are lower, it does not mean there is no toxic effect. Hydrocarbon exploration and production has occurred for many infauna generations at the Ixtoc site, so it is possible that organisms in this area can tolerate existing levels of PAH.

The macrofauna community exhibits signs of disturbance, but not at

all locations. Higher abundance and low diversity were found at station IXT (Fig. 6, Table 4). This combination of benthic metrics was also found in the severely and moderately impacted area around the DWH wellhead (Montagna et al., 2013; Washburn et al., 2017; Washburn et al., 2018). Impacts were classified as severe at locations within 3 km of the DWH wellhead, and as moderate within 15 km of the wellhead (Washburn et al. 2017). A 54% loss of macrofauna diversity and a 38% loss of meiofauna diversity were classified as severe effects (Montagna et al., 2013). This same trend was also seen four years after the spill when macrofauna where compared between impacted and non-impacted locations (Reuscher et al. 2017). Contaminant presence is also evident by sediment depth (Table 4). Overall, macrofauna abundance, diversity, and richness were highest in the top 3 cm. This is the typical vertical pattern because the superficial sediments have greater dissolved oxygen concentrations and food availability, particularly in the deep sea as in shallower depth zones (Giere, 2009; Montagna et al., 2017). When macrofauna community metrics by sediment depth were compared to PAH concentrations in this study, both potential toxic effects and enrichment effects were identified. A toxic effect is expected to cause a decrease in the abundance and diversity of the organisms (Jacobs, 1980; Sanders et al., 1980). At stations N1, N2 and W1 high PAH concentration corresponded to low abundance, richness, and diversity values at 3 – 5 cm sediment depth (Figs. 6,7). At station IXT the high PAH concentration corresponded to low diversity (Figs. 6,7), but not to low abundance and richness. Therefore, the macrofauna at station IXT are likely experiencing a moderate level of disturbance, which is likely due to both the Ixtoc spill and the legacy of pollution at the site.

For meiofauna the highest abundance and diversity were found at station IXT (Fig. 8, and Table 5). Organic enrichment is expected to result in high abundances of opportunistic and/or tolerant species, and thus low diversity in a contaminated area (Spies et al., 1988; Jewett et al., 1999; Washburn et al., 2017). However, at IXT there is both high abundance and high diversity. Increased meiofauna abundance and diversity was also observed in the presence of marine snow and petroleum during a microcosm experiment (Rohal et al., 2020). A similar increase in nematode abundance was found near petroleum platforms, which was attributed to increased food availability due to presence of fouling communities on platforms (Montagna and Harper, 1996). A higher Nematode to Copepod (NC) ratio is believed to be indicative of chemically and organically polluted locations, near seeps, sewage outfalls, and in low dissolved oxygen areas (Raffaelli and Mason, 1981; Shirayama and Ohta, 1990; Sellanes et al., 2010). The highest NC ratio was found at IXT (Table 6; Fig. 10), which could be indicating organic matter enrichment at this location. It must be noted that the IXT site is the shallowest, is nearest to land, and is in the midst of many other platforms, so the high NC could be due to one or more of all these drivers. Also, the NC ratio was the only benthic metric that correlated with PC1 (Table S1), which indicates that the NC ratio is high when the salinity, temperature, and TPAH concentration is high.

Overall, meiofauna abundance, diversity, and richness were highest in the top 1 cm as is expected (Table 5). However, significant station*section interactions occurred for nearly all meiofauna metrics including meiofauna diversity, meiofauna richness, copepod abundance, NC ratio, which indicates different processes are occurring at each station. This is likely attributed to ongoing changes in the surficial sediment influenced by ongoing petroleum production activity, and station depth. The NC ratio was much higher at station IXT in the 1 – 3 cm section compared to all other stations. High NC ratio values could be indications of chemical pollution because it was one of the key indicators of the DWH oil spill (Montagna et al., 2013, Baguley et al. 2015).

An Ixtoc-1 biogeochemical signal from foraminiferan isotopic data was found at stations W1 and W3 between 2.4 and 2.8 cm sediment depths (Table 2). This burial of the Ixtoc-1 chemicals does not mean that recovery has occurred for three reasons. First, sampling over a large spatial scale is key to assessing impacts so that the event is not indistinguishable from natural variability. Only seven stations were included in the current analysis therefore, it is likely that power to detect change caused by the Ixtoc-1 spill is low in the current study. Second, no Ixtoc-1 biogeochemical signal from foraminiferan isotopic data was detected at the two stations closest to the wellhead because the surface sediment appeared to be mixed and no evidence of lamination was found in the cores collected at those stations. But, TPAH concentration was highest at the 1 – 3 cm section at station IXT where an Ixtoc-1 signal would be expected based on sedimentation rates. Macrofauna diversity was lowest at the 1 – 3 cm section, which is unusual because the trend is for diversity/richness to decrease as depth in the sediment increases (Montagna et al., 2017). The NC ratio was much higher at station IXT in the 1 – 3 cm section compared to all other stations. High NC ratio values are indications of chemical pollution, low dissolved oxygen concentrations, and seepage and were one of the key indicators of the DWH oil spill (Montagna et al., 2013). TPAH concentration, macrofauna diversity with depth, and NC ratio with depth at station IXT suggest that recovery has not occurred after more than 30 years. Third, individual sediment depth profiles for each station indicate that different processes are happening at each location that can be related to the depth zone. The ongoing petroleum activity in the area has likely impacted each station to varying degrees and could be masking any residual Ixtoc-1 affects. At stations W1 and W3, where an Ixtoc-1 signal was found within the 1– 3 cm section there is a larger NC ratio when compared to station W2 which is at a comparable depth and had no Ixtoc-1 signal. Even though the number of copepods naturally decreases with sediment depth the differences between stations should be consistent across similar depths. The NC ratio high values at these stations likely indicates a continued Ixtoc-1 response based on observational evidence despite the lack of statistical validation.

In conclusion, the benthic community metrics around the site of the Ixtoc-1 oil spill supports the interpretation that recovery is in progress. The assumption is that recovery will occur when the contaminated sediment moves below the biologically active zone. Based on measurements made by Schwing and Machain-Castillo (2020, Table 2), an average Ixtoc-1 signal depth of 2.6 cm after 36 years yields a sedimentation rate is about 0.072 cm/year (range from 0.067 to 0.078). At the rate, it will take about 103 (range from 92 − 113) more years beyond 2015 until the benthic community has completely displaced the polluted sediment at more than 10 cm depth being then recovered from the Ixtoc-1 oil spill. The total will be 139 (range 128 – 149) years for recovery to occur. However, sedimentation rate is variable in space and time and the same rate will not apply to the area near the DWH wellhead. Sedimentation rates nearest the DWH wellhead, although deeper, range from 0.1 to 0.3 cm/year naturally with higher rates after the spill (Brooks et al., 2015) because of the closeness to the continental break and the occurrence on the continental slope and Mississippi fan. Based on an average rate of 0.2 cm/year the benthic community around the DWH well head will recover 50 (range 33–100) years after the well was capped.

CRediT authorship contribution statement

Melissa Rohal: Data curation, Formal analysis, Investigation, Writing - review & editing. **Noe Barrera:** Investigation, Writing - review & editing. **Elva Escobar-Briones:** Data curation, Investigation, Writing - review & editing. **Gregg Brooks:** Formal analysis, Data curation, Investigation. **David Hollander:** Conceptualization, Funding acquisition. **Rebekka Larson:** Data curation, Formal analysis, Investigation. **Paul A. Montagna:** Conceptualization, Data curation, Formal analysis, Investigation, Writing - review & editing, Supervision. **Marissa Pryor:** Investigation. **Isabel C. Romero:** Data curation, Formal analysis, Investigation, Writing - review & editing. **Patrick Schwing:** Data curation, Formal analysis, Investigation, Writing - review & editing.

Declaration of Competing Interest

The authors declare that they have no known competing financial interests or personal relationships that could have appeared to influence the work reported in this paper.

Acknowledgments

Research was partially supported by a grant from The Gulf of Mexico Research Initiative/C-IMAGE II, No. SA 15-16. Data are publicly available through the Gulf of Mexico Research Initiative Information & Data Cooperative (GRIIDC) at https://data.gulfresearchinitiative.org (doi: R4.x267.000:0116). This publication was made partially possible by the National Oceanic and Atmospheric Administration, Office of Education Educational Partnership Program award (NA16SEC4810009). Its contents are solely the responsibility of the award recipient and do not necessarily represent the official views of the U.S. Department of Commerce, National Oceanic and Atmospheric Administration. Research was also partially supported by a Harte Research Fellowship provided by the Harte Research Institute at Texas A&M University-Corpus Christi (TAMUCC). Many people at TAMUCC helped in completing this project. Elani Morgan (TAMUCC) helped with data management. Tiffany Hawkins, Courtney Armstrong, and Meagan Hardegree helped with sorting of the samples. Larry Hyde and Michael Reuscher helped with animal identification. Dr. Lee Smee and Dr. Jeff Baguley helped critique the manuscript.

Appendix A. Supplementary data

Supplementary data to this article can be found online at https://doi.org/10.1016/j.ecolind.2020.106593.

References

Adhikari, P.L., Wong, R.L., Overton, E.B., 2017. Application of enhanced gas chromatography/triple quadrupole mass spectrometry for monitoring petroleum weathering and forensic source fingerprinting in samples impacted by the Deepwater Horizon oil spill. Chemosphere 184, 939–950. https://doi.org/10.1016/j.chemosphere.2017.06.077.

Baguley, J.G., Montagna, P.A., Cooksey, C., Hyland, J.L., Bang, H.W., Morrison, C., Kamikawa, A., Bennetts, P., Saiyo, G., Parsons, E., Herdener, M., Ricci, M., 2015. Community response of the deep-sea soft-sediment metazoan meiofauna to the Deepwater Horizon blowout and oil spill. Mar. Ecol. Prog. Ser. 528, 127–140. https://doi.org/10.2254/meps11290.

Beriro, D.J., Vane, C.H., Cave, M.R., Nathanail, C.P., 2014. Effects of drying and comminution type on the quantification of Polycyclic Aromatic Hydrocarbons (PAH) in a homogenised gasworks soil and the implications for human health risk assessment. Chemosphere 111, 396–404. https://doi.org/10.1016/j.chemosphere.2014.03.077.

Brooks, G.R., Larson, R.A., Schwing, P.T., Romero, I., Moore, C., Reichart, G.J., Jilbert, T., Chanton, J.P., Hastings, D.W., Overholt, W.A., Marks, K.P., Kostka, J.E., Holmes, C.Q., Hollander, D., 2015. Sedimentation pulse in the NE Gulf of Mexico following the 2010 DWH blowout. PLoS ONE 10 (7), e0132341. https://doi.org/10.1371/journal.pone.0132341.

Carlisle, K.M., 2014. The Large Marine Ecosystem approach: Application of an integrated, modular strategy in projects supported by the Global Environment Facility. Environ. Develop. 11, 19–42. https://doi.org/10.1016/j.envdev.2013.10.003.

Daly, K., Passow, U., Chanton, J., Hollander, D., 2016. Assessing the impacts of oil-associated marine snow formation and sedimentation during and after the Deepwater Horizon oil spill. Anthropocene 13, 18–33. https://doi.org/10.1016/j.ancene.2016.01.006.

Danovaro, R. 2010. Methods for the Study of Deep-Sea Sediments, Their Functioning and Biodiversity, CRC Press, Boca Raton, Florida, USA.

DWH Natural Resource Trustees, 2016. Deepwater Horizon oil spill: Final programmatic damage assessment and restoration plan and final programmatic environmental impact statement. [cited 2016 April 5]. Available from: http://www.gulfspillrestoration.noaa.gov/wp-content/uploads/Chapter-2_Incident-Overview_508.pdf.

Giere, O., 2009. Meiobenthology the microscopic motile fauna of aquatic sediments, second ed. Springer-Verlag, Berlin.

Jernelöv, A., Lindén, O., 1981. A cast study of the World's largest oil spill. Ambio 10, 299-306. https://www.jstor.org/stable/4312725.

Jernelöv, A., 2010. The threats from oil spills: now, then, and in the future. Ambio 39, 353–366. https://doi.org/10.1007/s13280-010-0085-5.

Kennicutt II, M.C., Green, R.H., Montagna, P., Roscigno, P.F., 1996. Gulf of Mexico Offshore Operations Experiment (GOOMEX) Phase I: Sublethal responses to contaminant exposure – introduction and overview. Can. J. Fish. Aquat. Sci. 53, 2540–2553. https://doi.org/10.1139/cjfas-53-11-2540.

Long, E.R., Macdonald, D.D., Smith, S.L., Calder, F.D., Bin, C., Smith, S.L., 1995. Incidence of adverse biological effects within ranges of chemical concentrations in marine and estuarine sediments. Environ. Manage. 19, 81–97. https://doi.org/10.1007/BF02472006.

Jacobs, R.P.W.M., 1980. Effects of the 'Amoco Cadiz' oil spill on the seagrass community at Roscoff with special reference to the benthic infauna. Mar. Ecol. Prog. Ser. 2, 207-212. https://www.int-res.com/articles/meps/2/m002p207.pdf.

Jewett, S.C., Dean, T.A., Smith, R.O., Blanchard, A., 1999. 'Exxon Valdez' oil spill: impacts and recovery in the soft-bottom benthic community in and adjacent to eelgrass beds. Mar. Ecol. Prog. Ser. 185, 59–83. https://doi.org/10.3354/meps185059.

Montagna, P.A., Harper, D.E., 1996. Benthic infaunal long-term response to offshore production platforms in the Gulf of Mexico. Can. J. Fish. Aquat. Sci. 53, 2567–2588.

Montagna, P.A., Baguley, J.G., Cooksey, C., Hartwell, I., Hyde, L.J., Hyland, J.L., Kalke, R.D., Kracker, L.M., Reuscher, M., Rhodes, A.C.E., 2013. Deep-Sea Benthic Footprint of the Deepwater Horizon Blowout. PLoS One 8 (8), e70540. https://doi.org/10.1371/journal.pone.0070540.

Montagna, P.A., Baguley, J.G., Hsiang, C.Y., Reuscher, M.G., 2017. Comparisons of sampling methods for deep-sea infauna. Limnol. Oceanog. Meth. 15 (2), 166–183. https://doi.org/10.1002/ieam.1791.

Oil Spill Intelligence Report Volume III 1980 Center for Short-Lived Phenomena Cambridge, MA.

Passow, U., 2016. Formation of rapidly-sinking, oil-associated marine snow. Deep-Sea Res. II 129, 232–240. https://doi.org/10.1016/j.dsr2.2014.10.001.

Passow, U., Ziervogel, K., Asper, V., Diercks, A., 2012. Marine snow formation in the aftermath of the Deepwater Horizon oil spill in the Gulf of Mexico. Environ. Res. Lett. 7 (3), 035301. https://doi.org/10.1088/1748-9326/7/3/035301.

Raffaelli, D.G., Mason, C.F., 1981. Pollution monitoring with meiofauna, using the ratio of nematodes to copepods. Mar. Poll. Bull. 12, 158–163. https://doi.org/10.1016/0025-326X(81)90227-7.

Reuscher, M.G., Baguley, J.G., Conrad-Forrest, N., Cooksey, C., Hyland, J.L., Lewis, C., Montagna, P.A., Ricker, R.W., Rohal, M., Washburn, T., 2017. Temporal patterns of Deepwater Horizon impacts on the benthic infauna of the northern Gulf of Mexico continental slope. PLoS One 12 (6), e0179923. https://doi.org/10.1371/journalpone.0179923.

Rohal, M., Barrera, N., van Eenennaam, J.S., Foekema, E.M., Montagna, P.A., Murk, A.J., Pryor, M., Romero, I.C., 2020. The impact of experimental oil-contaminated marine snow on meiofauna. Mar. Poll. Bull. 150, 110656. https://doi.org/10.1016/j.marpolbul.2019.110656.

Romero, I.C., 2019. A high-throughput method (ASE-GC /MS/MS/MRM) for quantification of multiple hydrocarbon compounds in marine environmental samples. Mar. Technol. Soc. J. 52, 66–70. https://doi.org/10.4031/MTSJ.52.6.6.

Romero, I.C., Chanton, J.P., Roseheim, B.E., Radović, J.R., Schwing, P.T., Hollander, D.J., Larter, S.R., Oldenburg, T.B.P., 2020. Long-term preservation of oil spill events in sediments: the case for the Deepwater Horizon oil spill in the northern Gulf of Mexico (Chap. 17).). In: Murawski, S.A., Ainsworth, C., Gilbert, S., Hollander, D., Paris, C.B., Schlüter, M., Wetzel, D. (Eds.), Deep Oil Spills: Facts, Fate, Effects. Springer, Cham, Switzerland, pp. 285–300.

Romero, I.C., Schwing, P.T., Brooks, G.R., Larson, R.A., Hastings, D.W., Flower, B.P., Goddard, E.A., Hollander, D.J., 2015. Hydrocarbons in deep sea sediments following the 2010 Deepwater Horizon Blowout in the Northeast Gulf of Mexico. PLoS One 10 (5), e0128371. https://doi.org/10.1371/journal.pone.0128371.

Romero, I.C., Sutton, T., Carr, B., Quintana-Rizzo, E., Ross, S.W., Hollander, D.J., Torres, J.J., 2018. Decadal assessment of polycyclic aromatic hydrocarbons in mesopelagic fishes from the Gulf of Mexico reveals exposure to oil-derived sources. Environ. Sci. Technol. 52, 10985–10996. https://doi.org/10.1021/acs.est.8b02243.

Romero, I.C., Toro-Farmer, G., Diercks, A.R., Schwing, P.T., Muller-Karger, F., Murawski, S., Hollander, D.J., 2017. Large Scale deposition of weathered oil in the Gulf of Mexico following a deepwater oil spill. Environ. Pollut. 228, 179–189. https://doi.org/10.1016/j.envpol.2017.05.019.

Ryerson, T.B., Camilli, R., Kessler, J.D., Kujawinski, E.B., Reddy C.M., 2012. Chemical data quantify Deepwater Horizon hydrocarbon flow rate and environmental distribution. Proc. Natl. Acad. Sci. 109, 20246-20253. www.pnas.org/cgi/doi/10.1073/pnas.1110564109.

Sanders, H.L, Grassle, J.F., Hampson, G.R., Morse, L.S., Garner-Price, S., Jones, C.C., 1980. Anatomy of an oil spill: long-term effects from the grounding of the barge Florida off west-Falmouth, Massachusetts. J. Mar. Res. 38, 265-380. https://darchive.mblwhoilibrary.org/bitstream/handle/1912/3474/J%20marine%20research%20v38%201980.pdf?sequence=1&isAllowed=y.

SAS Institute Inc., 2017. SAS/STAT® 14.3 Users Guide. Cary, North Carolina, USA.

Schwing, P.T., Brooks, G.R., Larson, R.A., O'Malley, B.J., Hollander, D.J., 2017. Constraining the spatial extent of the Marine Oil Snow Sedimentation and Accumulation (MOSSFA) following the DWH event using a $^{210}Pb_{xs}$ inventory approach. Env. Sci. Tech. 51, 5962–5968. https://doi.org/10.1021/acs.est.7b00450.

Schwing, P.T., Chanton, J.P., Romero, I.C., Hollander, D.J., Goddard, E.A., Brooks, G.R., Larson, R.A., 2018. Tracing the incorporation of carbon into benthic foraminiferal calcite following the Deepwater Horizon event. Env. Poll. 237, 424–429.

Schwing P.T., Machain-Castillo, M.L., 2020a. Impact and resilience of benthic foraminifera in the aftermath of the Deepwater Horizon and Ixtoc 1 oil spills (Chap. 23). In: Murawski, S.A., Ainsworth, C., Gilbert, S., Hollander, D., Paris, C.B., Schlüter, M., Wetzel, D. (Eds.), Deep Oil Spills: Facts, Fate, Effects. Springer, Cham, Switzerland, pp. 374–387.

Schwing, P.T., Machain-Castillo, M.L., Brooks, G.R., Larson, R.A., Fillingham, J.N., Sanchez-Cabeza, J.A., Ruiz-Fernández, A.C., Hollander, D.J., (In Prep). Multi-proxy assessment of recent regional-scale events recorded in Southern Gulf of Mexico

sediments.
Schwing, P.T., Montagna, P.A., Machain-Castillo, M.L., Escobar-Briones, E., Rohal, M., 2020b. Benthic faunal baselines in the Gulf of Mexico: A precursor to evaluate future impacts (Chap. 6). In: Murawski, S.A., Ainsworth, C., Gilbert, S., Hollander, D., Paris, C.B., Schlüter, M., Wetzel, D. (Eds.), Scenarios and Responses to Future Deep Oil Spills. Springer, Cham, Switzerland, pp. 96–108.
Sellanes, J., Neira, C., Quiroga, E., Teixido, N., 2010. Diversity Patterns along and across the Chilean margin: a continental slope encompassing oxygen gradients and methane seep benthic habitats. Mar. Ecol. 31, 111–124.
Shirayama, Y., Ohta, S., 1990. Meiofauna in a cold-seep community off Hatsushima, central Japan. J. Oceanogr. Soc. Jpn. 46, 118–124.
Sorensen, L., Meier, S., Mjos, S.A., 2016. Application of gas chromatography/tandem mass spectrometry to determine a wide range of petrogenic alkylated polycyclic aromatic hydrocarbons in biotic samples. Rapid Commun. Mass Spectrom. 30, 2052–2058. https://doi.org/10.1002/rcm.7688.
Spies, R.B., Hardin, D.D., Toal, J.P., 1988. Organic enrichment or toxicity? A comparison of the effects of kelp and crude oil in sediments on the colonization and growth of benthic infauna. J. Exp. Mar. Biol. Ecol. 124, 261–282. https://doi.org/10.1016/0022-0981(88)90175-X.
Sun, S., Hu, C., Tunnell Jr., J.W., 2015. Surface oil footprint and trajectory of the Ixtoc-1 oil spill determined from Landsat/MSS and CZCS observations. Mar. Poll. Bull. 101, 643–1641. https://doi.org/10.1016/j.marpolbul.2015.10.036.
D.L. Valentine G.B. Fisher S.C. Bagby R.K. Nelson C.M. Reddy S.P. Sylva M.A. Woo Fallout plume of submerged oil from Deepwater Horizon Proc. Nat. Acad. Sci. 111 45 2014 15906–15911. www.pnas.org/cgi/doi/10.1073/pnas.1414873111.
Van Eenennaam, J.S., Rahsepar, S., Radović, J.R., Oldenburg, T.B.P., Wonink, J., Langenhoff, A.A.M., Murk, A.J., Foekema, E.M., 2018. Marine snow increases the adverse effects of oil on benthic invertebrates. Mar. Pollut. Bull. 126, 339–348. https://doi.org/10.1016/j.marpolbul.2017.11.028.
Vonk, S.M., Hollander, D.J., Murk, A.J., 2015. Was the extreme and wide-spread marine snow sedimentation and flocculent accumulation (MOSSFA) event furing the Deepwater Horizon blow-out unique? Mar. Poll. Bull. 100, 5–12. https://doi.org/10.1016/j.marpolbul.2015.08.023.
Wade, T.L., Soliman, Y., Sweet, S.T., Wolff, G.A., Presley, B.J., 2008. Trace elements and polycyclic aromatic hydrocarbons (PAHs) concentrations in deep Gulf of Mexico sediments. Deep-Sea Res. Part II 55, 2585–2593. https://doi.org/10.1016/j.dsr2.2008.07.006.
Washburn, T., Rhodes, A.C.E., Montagna, P.A., 2016. Benthic taxa as potential indicators of a deep-sea oil spill. Ecol. Ind. 71, 587–597. https://doi.org/10.1016/j.ecolind.2016.07.045.
Washburn, T.W., Reuscher, M.G., Montagna, P.A., Cooksey, C., Hyland, J.L., 2017. Macrobenthic community structure in the deep Gulf of Mexico one year after the Deepwater Horizon blowout. Deep-Sea Res. Part I 127, 21–30. https://doi.org/10.1016/j.dsr.2017.06.001.
Washburn, T.W., Demopoulos, A.W.J., Montagna, P.A., 2018. Macrobenthic infaunal communities associated with deep-sea hydrocarbon seeps in the northern Gulf of Mexico. Mar. Ecol. Evolut. Perspect. 39, e12508. https://doi.org/10.1111/maec.12508.
Yáñez-Arancibia, A., Day, J.W., 2004. The Gulf of Mexico: towards an integration of coastal management with large marine ecosystem management. Oce Coast. Manage. 47, 537–563. https://doi.org/10.1016/j.ocecoaman.2004.12.001.
Ziervogel, K., McKay, L., Rhodes, B., Osburn, C.L., Dickson-Brown, J., Arnosti, C., Teske, A., 2012. Microbial activities and dissolved organic matter dynamics in oil-contaminated surface seawater from the Deepwater Horizon oil spill site. PLoS One 7 (4), e34816. https://doi.org/10.1371/journal.pone.00.